Electronic Supplementary Information

Multiple aggregates from multiple polymorphs: structural and mechanistic insight into organic dye aggregates

David T. Hogan and Todd C. Sutherland*

Email: todd.sutherland@ucalgary.ca

Table of Contents

Section 1	Aggregate Preparation and Experimental Considerations	2
Section 2	Water Fraction Series Measured by Emission Spectroscopy	4
Section 3	Photographs of Aggregate Suspensions	6
Section 4	Water Fraction Series Measured by UV-visible Absorbance Spectroscopy	7
Section 5	Scattering Deconvolution Methods	9
Section 6	Scanning Electron Microscopy	12
Section 7	Dynamic Light Scattering	18
Section 8	Ageing Experiments	22
Section 9	Thermal Treatment Experiments	23
Section 10	Variable Solvent Composition Experiments	25
Section 11	Time-resolved emission	26
Section 12	Polymorphs orange and yellow crystal structures and thermal properties.	33
Section 13	References	35

Section 1 Aggregate Preparation and Experimental Considerations

Dioxane was purchased from Sigma Aldrich (ACS reagent grade ≥ 99.0%) and water was purified through an EMD 18.2 MΩ Milli-Q water purifier system.

Synthesis of **1** was performed according to Hogan, D. T.; Gelfand, B. S.; Spasyuk, D. M.; Sutherland, T. C. *Mater. Chem. Front.* **2020**, *4*, 268-276.[1]

To make aggregates at 10 μM final concentration, a 100 μM stock solution of **1** in dioxane was prepared. Light sonication for 30 seconds quickens dissolution. To prepare the aggregated solutions for measurement, 200 μL of this solution were added to a cuvette. This was diluted to 2 mL with dioxane for the f_w 0% sample. To prepare the vials containing water, 200 μL of Milli-Q water (each 200 μL = 10 volume%) were quickly added to the tube to replace 200 μL of dioxane. This works out as follows:

f_w 0% – 200 μL stock, 1.8 mL dioxane

f_w 10% – 200 μL stock, 1.6 mL dioxane, 200 μL water

f_w 20% – 200 μL stock, 1.4 mL dioxane, 400 μL water

f_w 30% – 200 μL stock, 1.2 mL dioxane, 600 μL water

f_w 40% – 200 μL stock, 1.0 mL dioxane, 800 μL water

f_w 50% – 200 μL stock, 800 μL dioxane, 1.0 mL water

f_w 60% – 200 μL stock, 600 μL dioxane, 1.2 L water

f_w 70% – 200 μL stock, 400 μL dioxane, 1.4 mL water

f_w 80% – 200 μL stock, 200 μL dioxane, 1.6 mL water

f_w 90% – 200 μL stock, 1.8 mL water

To conduct the ageing experiment, aggregate suspensions were prepared in the usual way and measured within 1 minute of preparation. The aggregates were then stored at room temperature in the dark and measured every 24 hours.

To conduct the heating experiments, the f_w 60% and 90% aggregate suspensions were prepared in the usual way and measured within 1 minute preparation. The cuvette was then put into the Peltier heating block set to 90 °C (85.63 °C solution temp.) and the spectra were recorded every 10 minutes. Once complete, the heating block was set to 20 °C (20.29 °C solution temp) and the spectra were recorded once again.

To conduct the experiments where f_w 60%→90%, a f_w 60% aggregate suspension was prepared in the usual way and measured within 1 minute of preparation. The suspension was then transferred to a 20 mL vial, 0.15 mL of 500 μM **1** stock (dioxane) were added to maintain concentration, then 7.35 mL of Milli-Q water were added. The suspension was swirled, and spectra were recorded every 10 minutes.

To conduct experiments where f_w 90%→60%, a f_w 90% aggregate suspension was prepared in the usual way and measured within 1 minute of preparation. 0.1 mL of 100 μM **1** stock were added to maintain concentration, then 0.9 mL of dioxane were added. The suspension was swirled, then absorption spectra were recorded in cycle mode at 600 nm/min between 350-700 nm. A separate solution was used to record the emission spectra on cycle mode at 100 nm/min between 470-840 nm.

Relative emission quantum yield determination:[2] Relative emission quantum yields were obtained using coumarin 6 (Φ_{em} = 0.78)[3] in absolute ethanol as the emission standard, excited at 420 nm. The absorbance at 420 nm was less than 0.1 arbitrary units. Samples of aggregates were prepared according to the above procedure and measured without dilution. To account for light scattering, the ratio of the absorption to the total light extinction at 420 nm was obtained from the scattering deconvolution procedure described in Section 5, and then multiplied by the absorbance measured on a spectrophotometer.

Table S1. Summary of relative emission quantum yields for each water fraction.

f_w	Φ_{em} Uncorr.	Φ_{em} Corr.*	f_w	Φ_{em} Uncorr.	Φ_{em} Corr.*
10	0.236	0.236	**60**	0.009	0.017
20	0.005	0.005	**70**	0.008	0.017
30	0.002	0.002	**80**	0.008	0.013
40	0.001	0.001	**90**	0.007	0.007
50	0.001	0.001			

*Corrected emission quantum yields account for scattering.

Section 2 Water Fraction Series Measured by Emission Spectroscopy

Emission spectroscopy was performed using a Jasco FP-6600 emission spectrophotometer on medium sensitivity mode collecting a single scan. The excitation wavelength for all aggregates was 460 nm, excitation bandwidth was 10 nm, emission bandwidth of 6 nm (data points +/- 3 nm), integration time of 0.2 seconds, data pitch of 1 nm, scanning speed of 200 nm/minute.

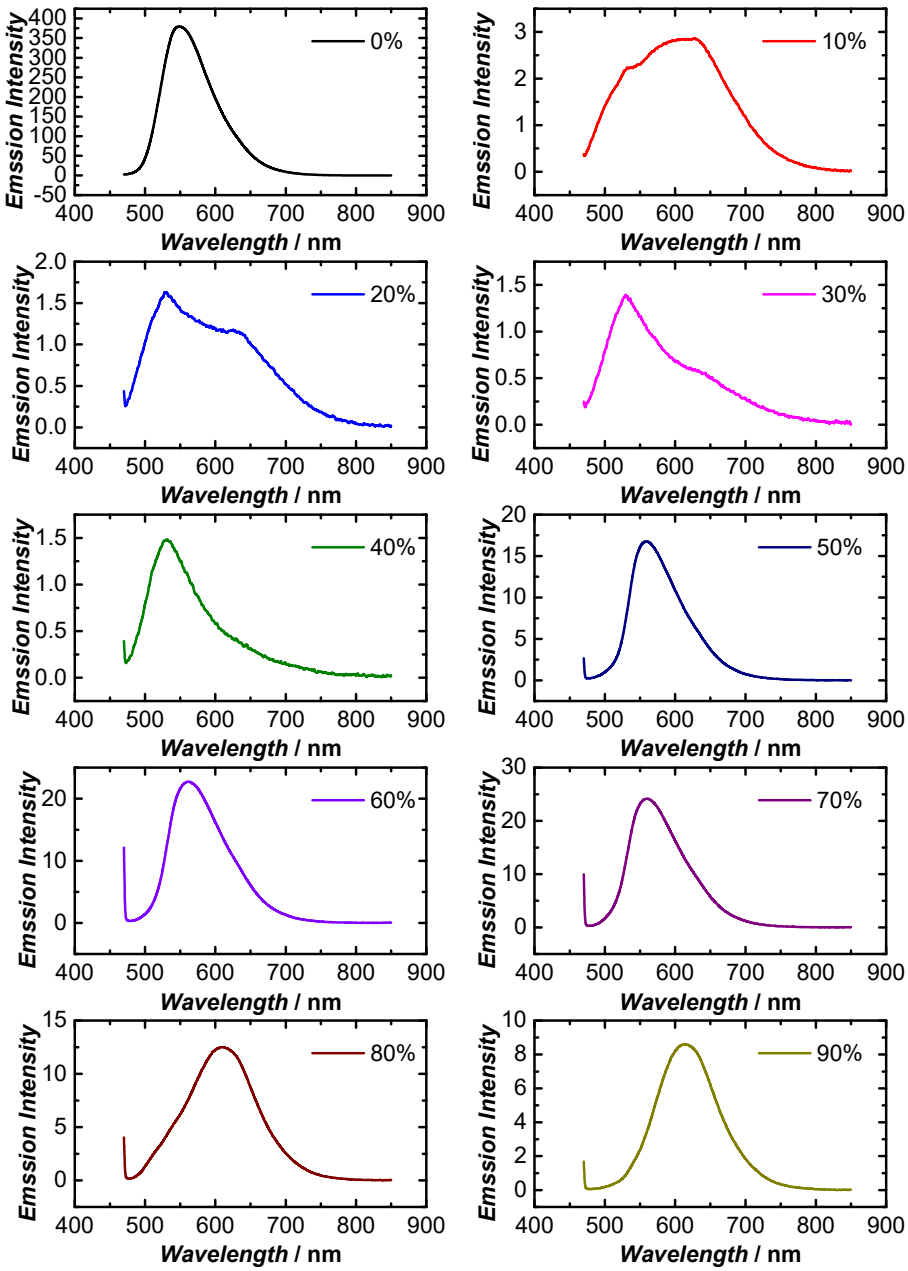

Figure S1. Non-normalized emission spectra (λ_{exc}= 460 nm) of solutions of **1** with different water fractions labelled in each plot. Replicate 1.

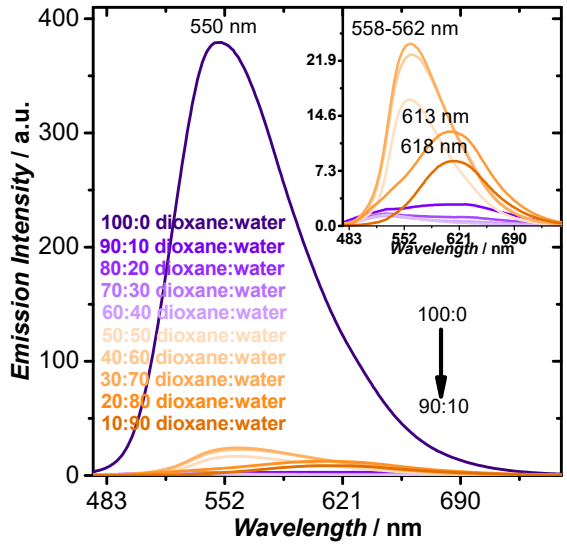

Figure S2.a Non-normalized emission spectra (λ_{exc}= 460 nm) of solutions of **1** with different water fractions labelled in each plot. Replicate 2.

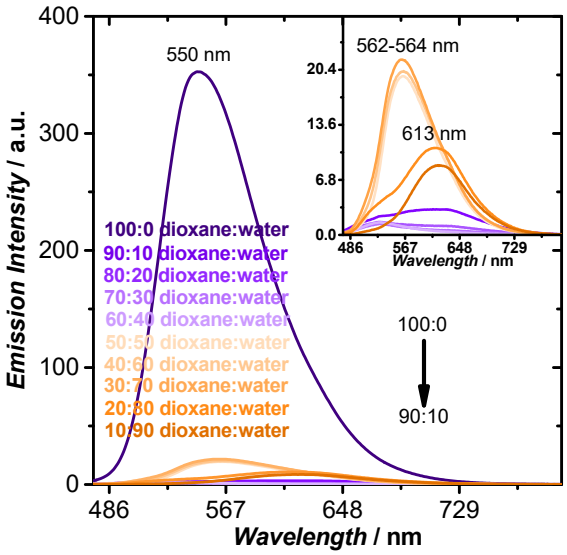

Figure S2.b Non-normalized emission spectra (λ_{exc}= 460 nm) of solutions of **1** with different water fractions labelled in each plot. Replicate 3.

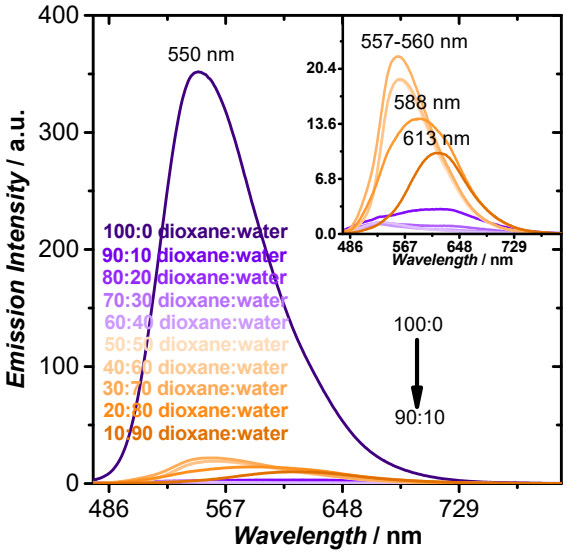

Figure S3. Non-normalized emission spectra (λ_{exc}= 460 nm) of solutions of **1** with different water fractions labelled in each plot. Replicate 4.

Section 3 Photographs of Aggregate Suspensions

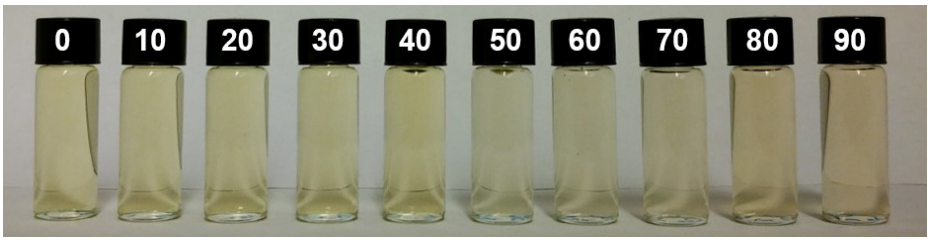

Figure S4. Photographs of aggregate suspensions from f_w 0-90% under visible light.

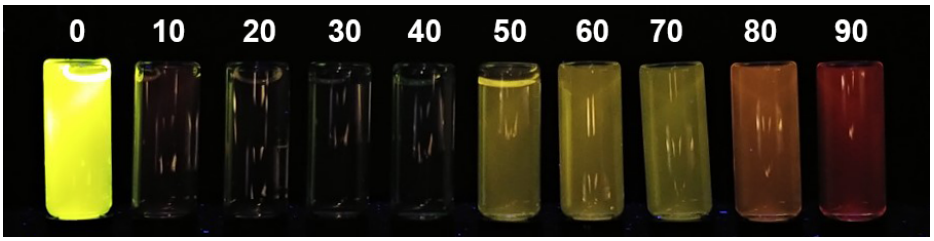

Figure S5. Photographs of aggregate suspensions from f_w 0-90% under 365 nm light

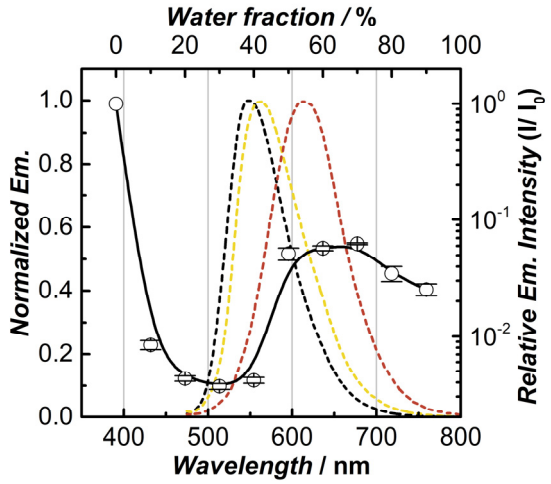

Figure S6. Normalized emission spectra of 10 μM **1** in dioxane solution with f_w 0% (black, λ_{exc}= 450 nm), **agg-Y** f_w 60% (yellow, λ_{exc}= 460 nm), and **agg-O** f_w 90% (orange, λ_{exc}= 460 nm); On the same set of axes, the relative emission intensity of the aggregates is plotted as a function of solution water fraction with error bars for 2 standard deviations.

Section 4 Water Fraction Series Measured by UV-visible Absorbance Spectroscopy

UV-visible absorption spectroscopy was performed using a Varian Cary 5000 UV-visible-NIR spectrophotometer in dual beam mode with spectral band width 2.0 nm, resolution 0.5 nm, scan speed 300 nm/min and averaging time 0.1 s, source change at 600 nm and UV-lamp change at 350 nm Solutions were measured at 298 K unless otherwise stated, and continuously referenced against blank solvent in quartz 10 mm path length cuvettes. For measurement at variable temperature, cuvettes were placed inside a 6x6 Varian Cary multicell Peltier block sample compartment, and the temperature was monitored using a Varian Cary Series II probe inserted into a cuvette of water-dioxane that was outside of the light path.

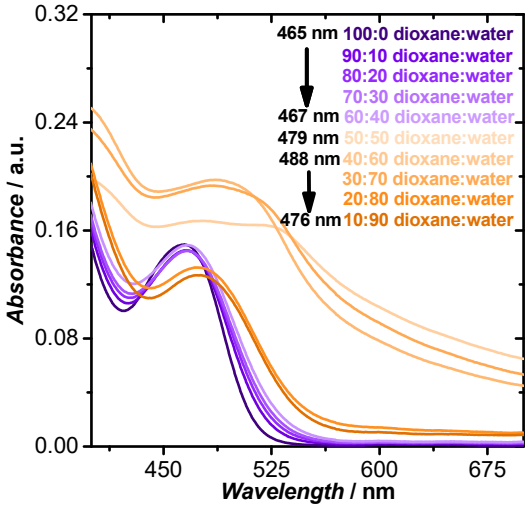

Figure S7.a Non-normalized Absorbance plots of **1** (10 μM) with varying f_w indicated in legend. Replicate 1.

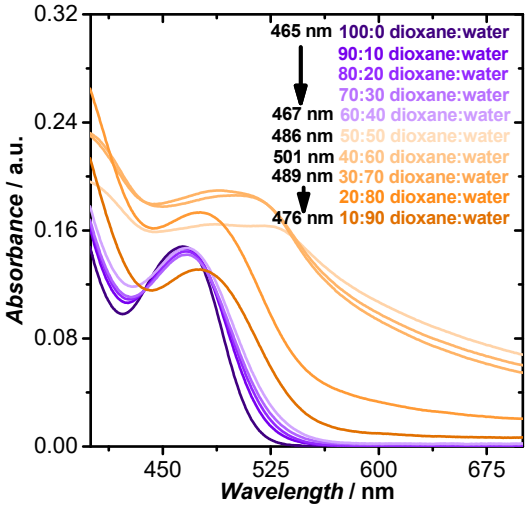

Figure S7.b Non-normalized Absorbance plots of **1** (10 μM) with varying f_w indicated in legend. Replicate 2.

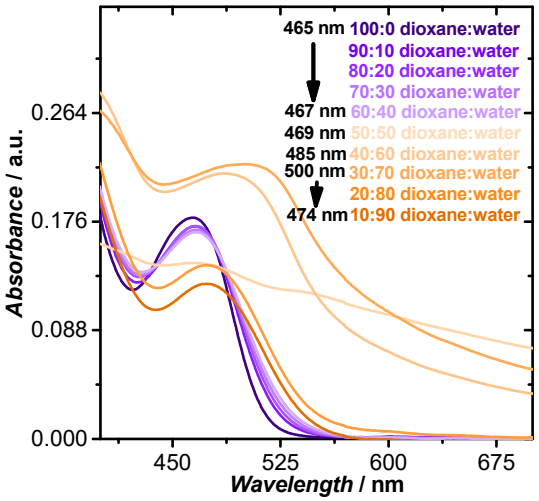

Figure S8.a Non-normalized Absorbance plots of **1** (10 μM) with varying f_w indicated in legend. Replicate 3.

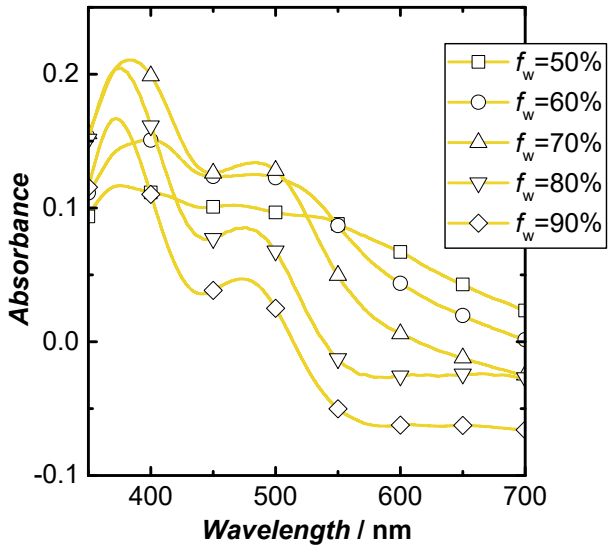

Figure S8.b Non-normalized Absorbance plots of **1** (10 μM) with varying f_w indicated in legend. Replicate 4.

Section 5 Scattering Deconvolution Methods

We followed the approach of Heyne and coworkers.[4–6]

The transmitted light (I_T) that passes through a cuvette containing particulate matter in suspension consists of the incident light (I_0), minus the light that is reflected from the cuvette walls (I_R, negligible in spectroscopic quartz), light that is absorbed by the particulate (I_A) and light that is scattered by the particulate (I_S). This is given by equation S1 below:

$$I_T = I_0 - I_A - I_S \qquad \textbf{(S1)}$$

The light that reaches the detector in a UV-visible spectrophotometer is largely transmitted light, due to the non-reflective coating inside the sample compartment. Thus, the scattered light never makes it to the detector, and the resulting absorbance spectrum consists of absorbed as well as scattered light. However, the reflective coating inside the integrating sphere of an emission spectrophotometer means that the scattered light can reach the detector, so any light that is lost is due exclusively to absorption by the particulate.

The baselines of blank dioxane-water mixtures of varying f_w were acquired on a Varian Cary 50 absorption spectrophotometer. For scattering deconvolution, an Edinburgh FLS900 emission spectrophotometer equipped with xenon lamp and a F-M01 integrating sphere assembly were used. The excitation and emission wavelengths were both set to 468 nm (peak output of Xe lamp), the emission slit was set to 1 nm and excitation was set to 2.8 nm, the combination which maximized the photons reaching the detector without saturation. A synchronous scan was then performed from 300-800 nm, with a 1 nm step height, 0.5 s dwell time averaging over 3 scans on blank dioxane-water mixture, and then the **1** aggregate sample. The true absorption spectrum of the aggregates was then found by subtracting the aggregate spectrum from the blank spectrum, using a feature of the F900 software by Edinburgh Instruments.

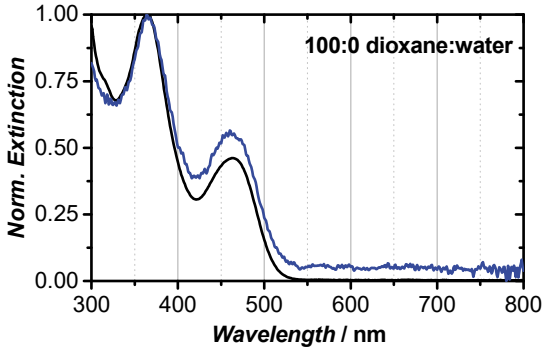

Figure S9.a Normalized absorbance of **1** (10 μM) in dioxane (f_w 0%). The black line is the absorbance spectrum, and the blue line is the scatter-corrected spectrum.

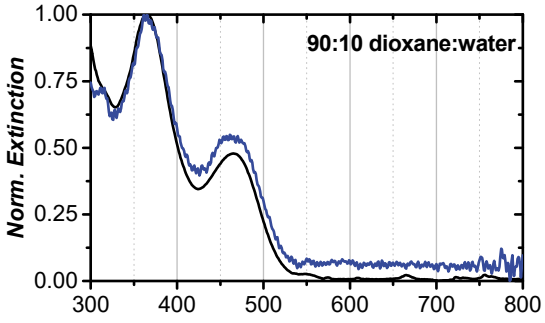

Figure S9.b Normalized absorbance of **1** (10 μM) in dioxane:water (f_w 10%). The black line is the absorbance spectrum, and the blue line is the scatter-corrected spectrum.

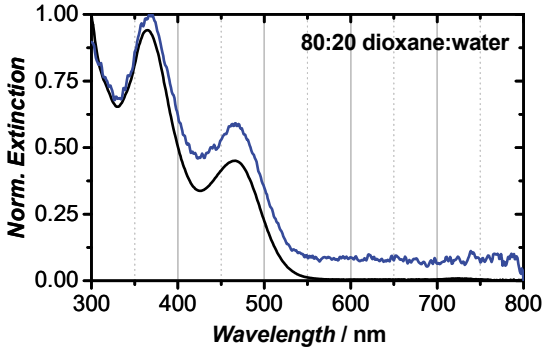

Figure S10.a Normalized absorbance of **1** (10 μM) in dioxane:water (f_w 20%). The black line is the absorbance spectrum, and the blue line is the scatter-corrected spectrum.

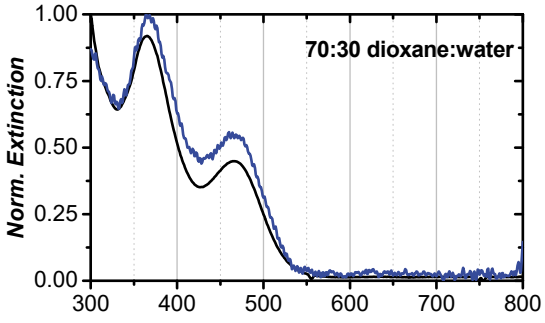

Figure S10.b Normalized absorbance of **1** (10 μM) in dioxane:water (f_w 30%). The black line is the absorbance spectrum, and the blue line is the scatter-corrected spectrum.

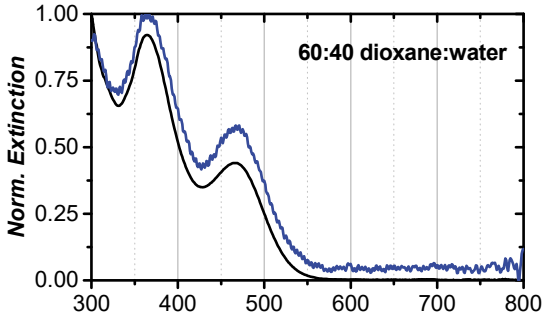

Figure S11.a Normalized absorbance of **1** (10 μM) in dioxane:water (f_w 40%). The black line is the absorbance spectrum, and the blue line is the scatter-corrected spectrum.

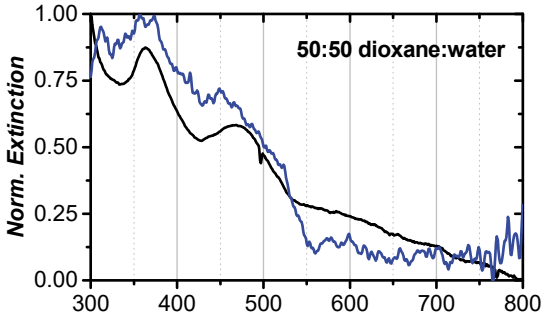

Figure S11.b Normalized absorbance of **1** (10 μM) in dioxane:water (f_w 50%). The black line is the absorbance spectrum, and the blue line is the scatter-corrected spectrum.

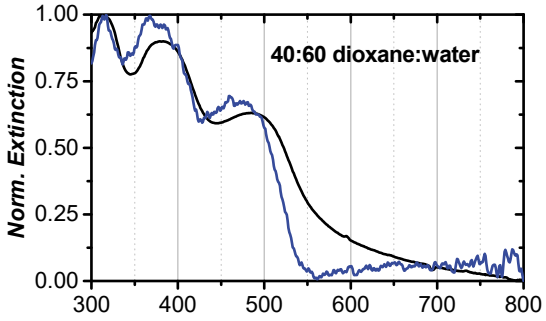

Figure S12.a Normalized absorbance of **1** (10 μM) in dioxane:water (f_w 60%). The black line is the absorbance spectrum, and the blue line is the scatter-corrected spectrum.

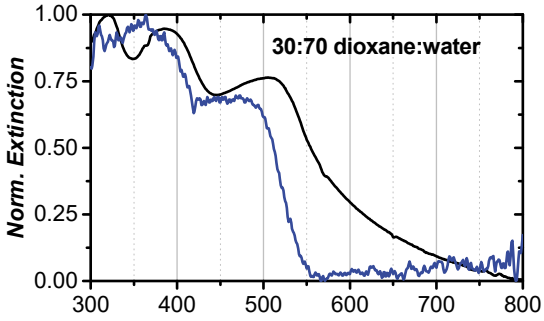

Figure S12.b Normalized absorbance of **1** (10 μM) in dioxane:water (f_w 70%). The black line is the absorbance spectrum, and the blue line is the scatter-corrected spectrum.

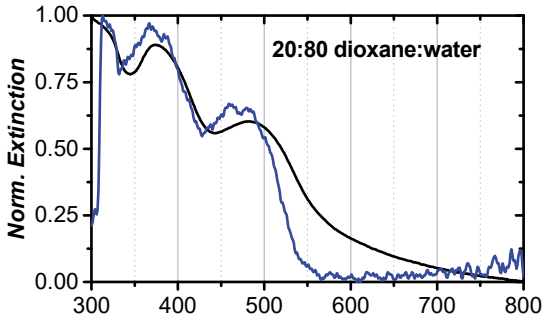

Figure S13.a Normalized absorbance of **1** (10 μM) in dioxane:water (f_w 80%). The black line is the absorbance spectrum, and the blue line is the scatter-corrected spectrum.

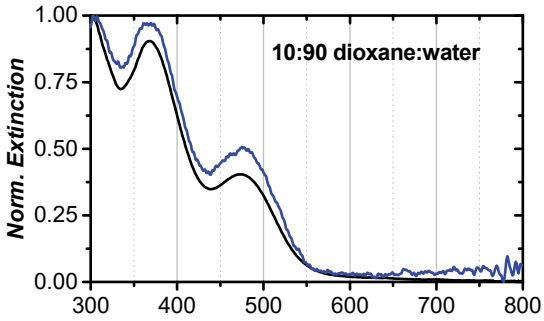

Figure S13.b Normalized absorbance of **1** (10 μM) in dioxane:water (f_w 90%). The black line is the absorbance spectrum, and the blue line is the scatter-corrected spectrum.

Section 6 Scanning Electron Microscopy

Samples were prepared for SEM in the following manner. Once the aggregate suspension had been prepared in the usual way, a 1 cm square of Si (100) wafer was placed onto a Laurell Technologies model WS-400B-6NPB/LITE/AS spin coater and spun at 5000 rpm. 1 mL of isopropanol (Sigma Aldrich ≥99.5%) was deposited to degrease the surface, and the wafer was allowed to spin dry for 10 seconds before 1 drop of aggregate suspension was added by Pasteur pipet, and the wafer was spun for an additional 10 seconds. The coated Si wafer was adhered with carbon tape to an aluminium stub, then electron micrographs were collected on a Zeiss Sigma VP scanning electron microscope with an EHT of 2 kV; working distances (W.D.) are marked on each micrograph.

Feret's Diameter was used for ImageJ (v 1.53p) analysis - The longest distance between any two points along the selection boundary, also known as maximum caliper. Uses the Feret heading. FeretAngle (0-180 degrees) is the angle between the Feret's diameter and a line parallel to the x-axis of the image. MinFeret is the minimum caliper diameter. The starting coordinates of the Feret's diameter (FeretX and FeretY) are also displayed. The DrawFeretDiameter macro draws the Feret's diameter of the current selection.

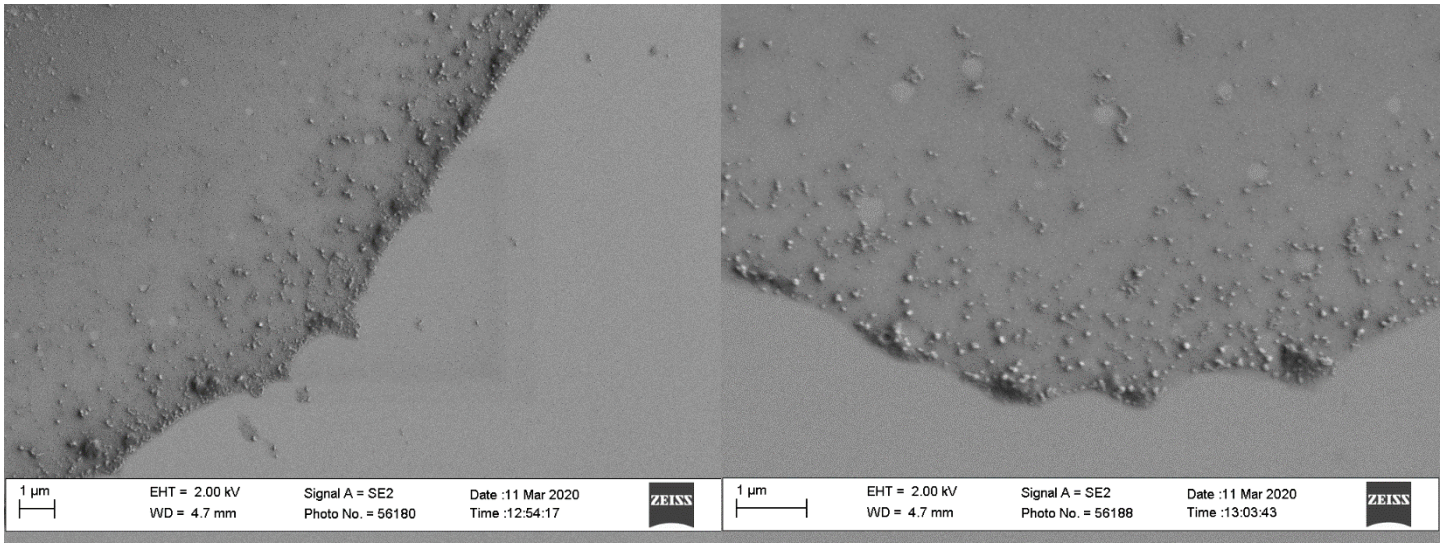

Figure S14. Electron micrographs of a blank dioxane-water mixture with f_w 50% using the secondary electron detector.

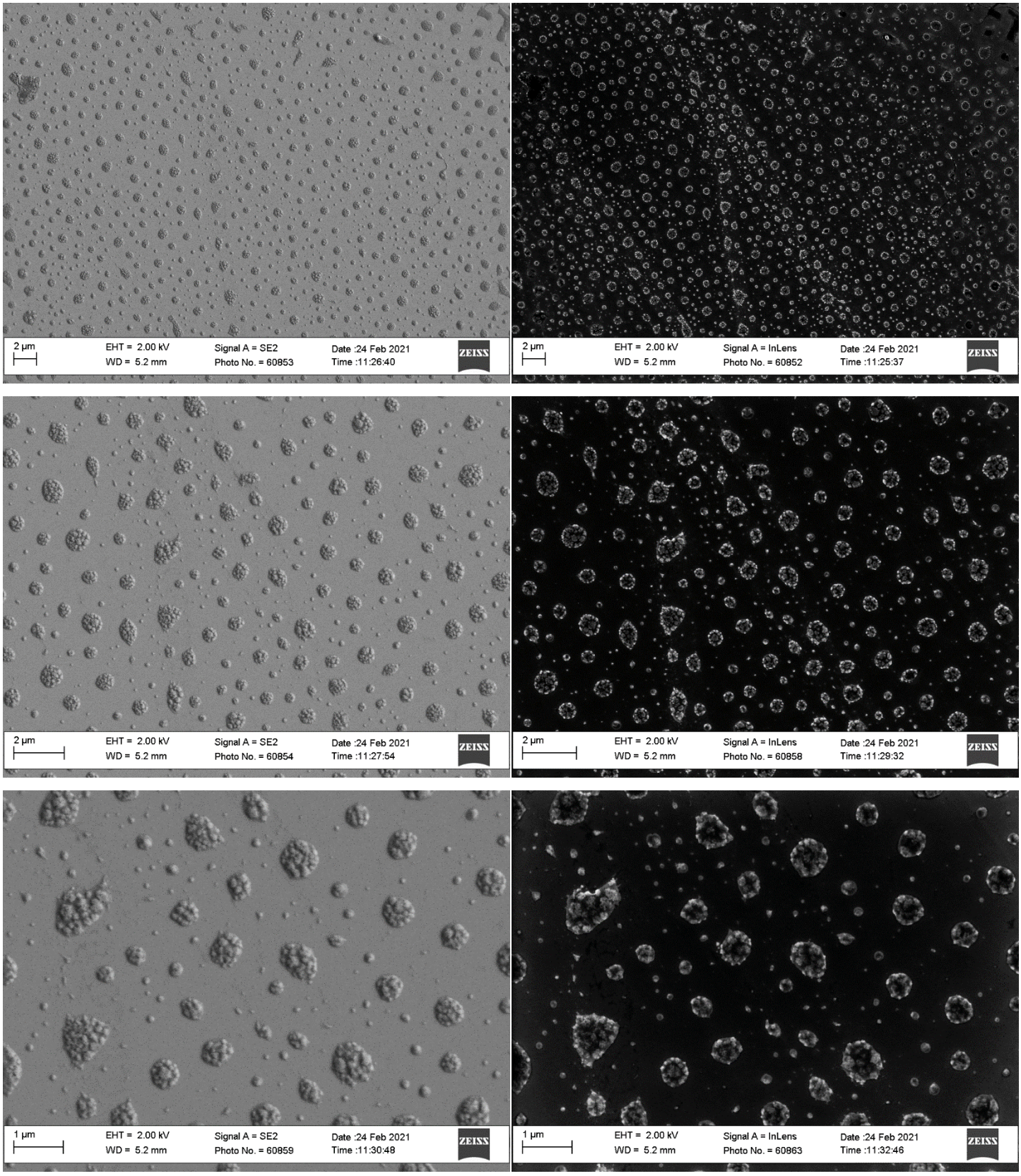

Figure S15. Electron micrographs of **1** aggregates at f_w 60% using the secondary electron (left) and in-lens detectors (right).

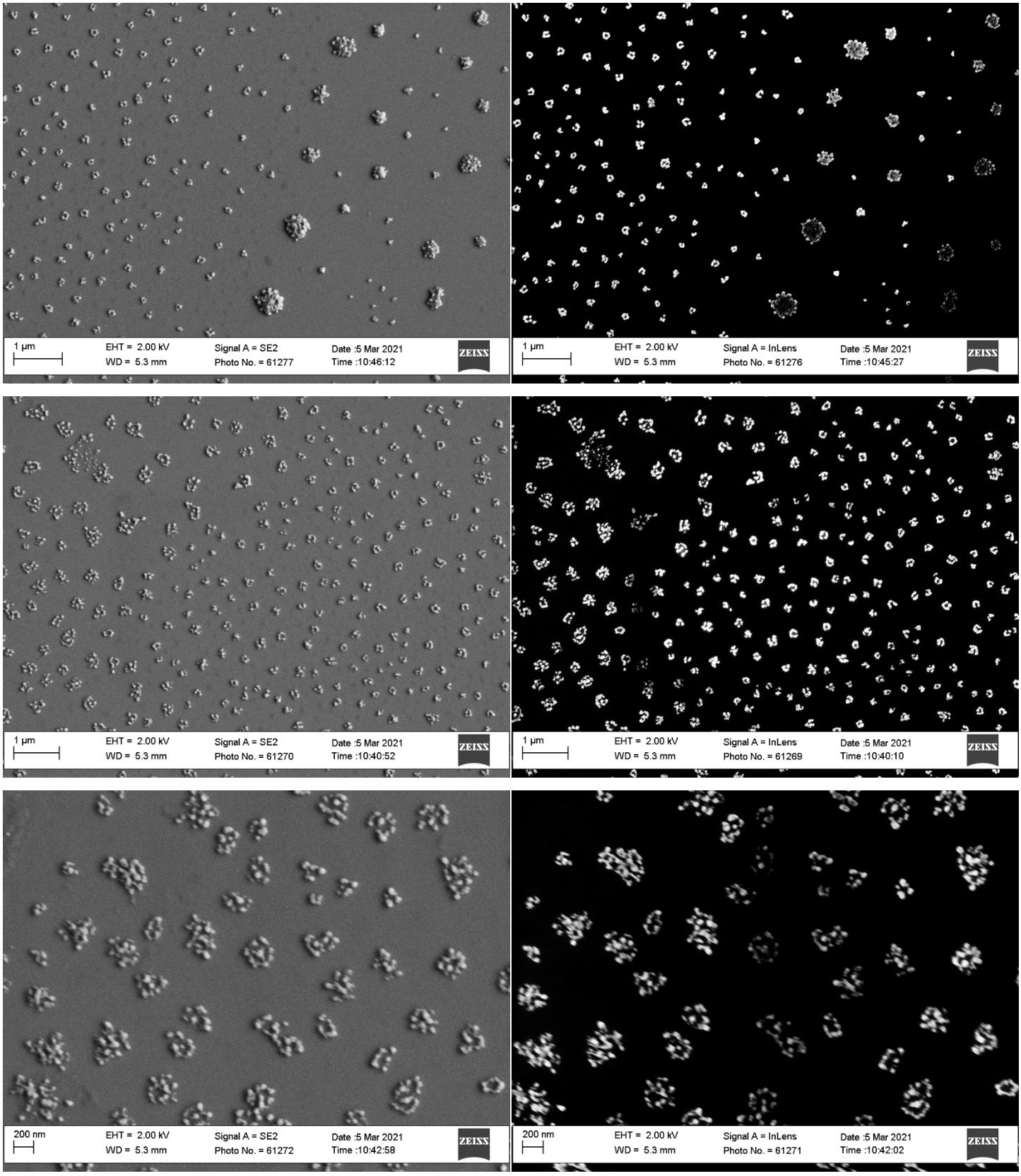

Figure S16. Electron micrograph of **1** aggregates f_w 70% using the secondary electron (left) and in-lens detectors (right).

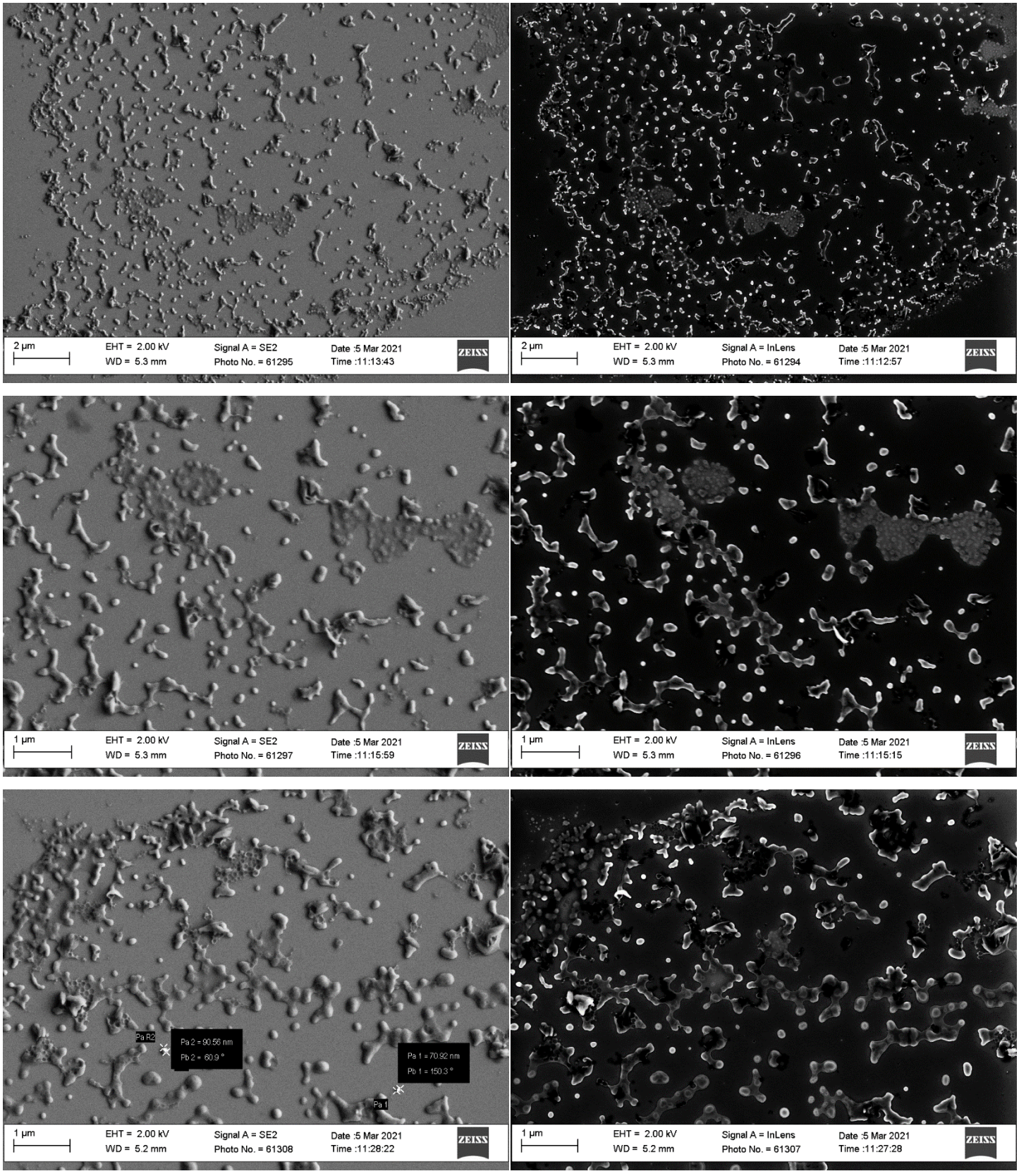

Figure S17. Electron micrograph of **1** aggregates f_w 80% using the secondary electron (left) and in-lens detectors (right).

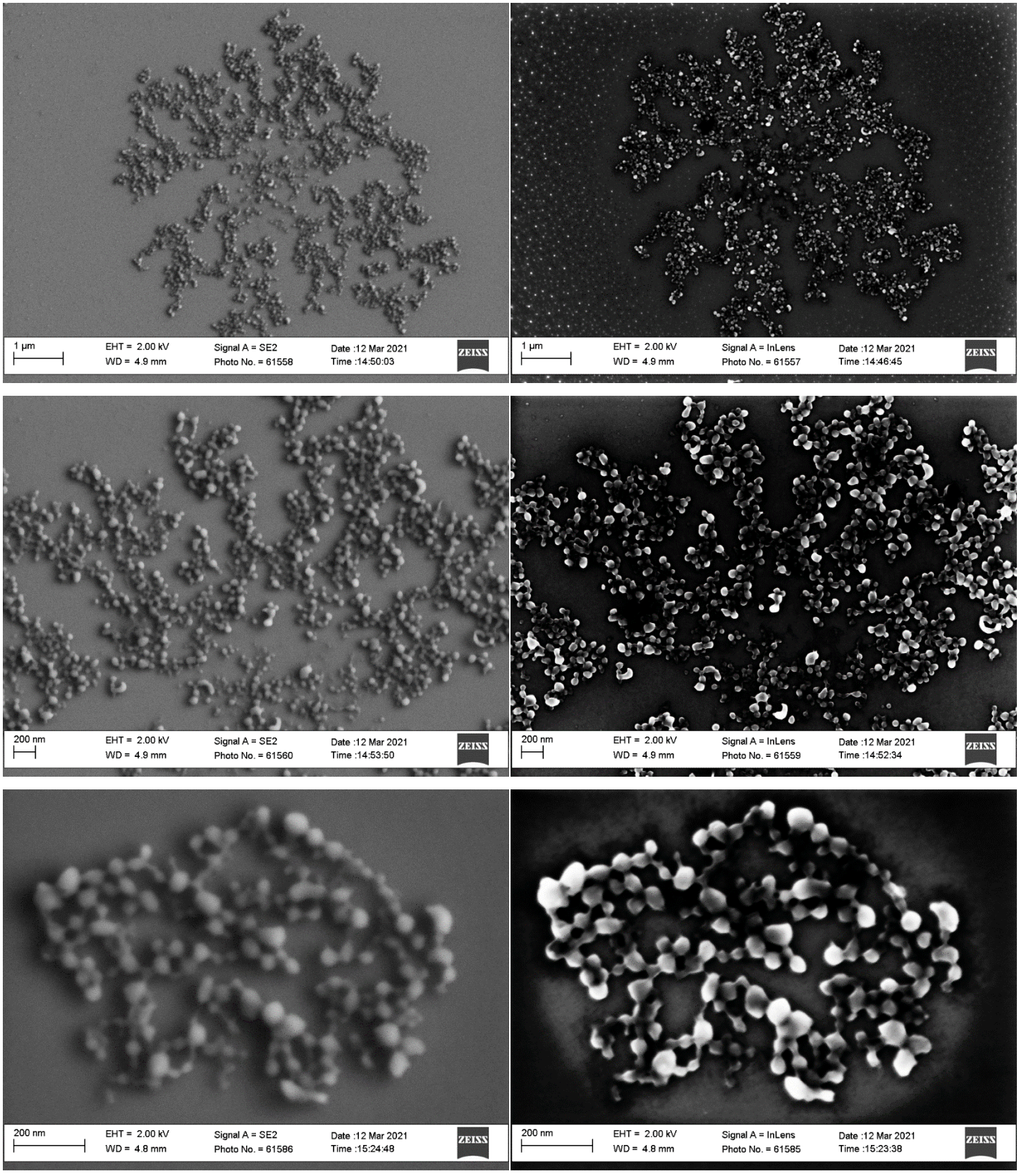

Figure S18. Electron micrograph of **1** aggregates f_w 90% using the secondary electron (left) and in-lens detectors (right).

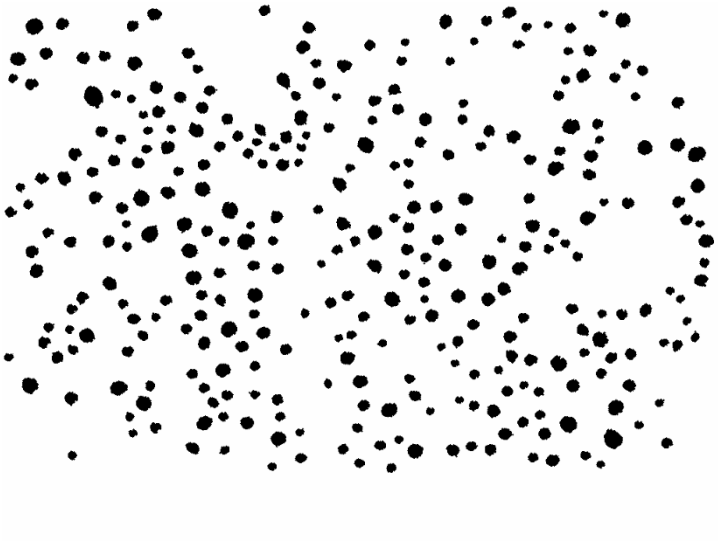

Figure S19. Using ImageJ v1.53p software, the following particles were counted/extracted from Photo No. 60853, shown above, using default threshold settings and the included 'Analyze Particles' function. The particles identified by ImageJ were used to create the diameter distribution plots of the aggregates in Figure 4.

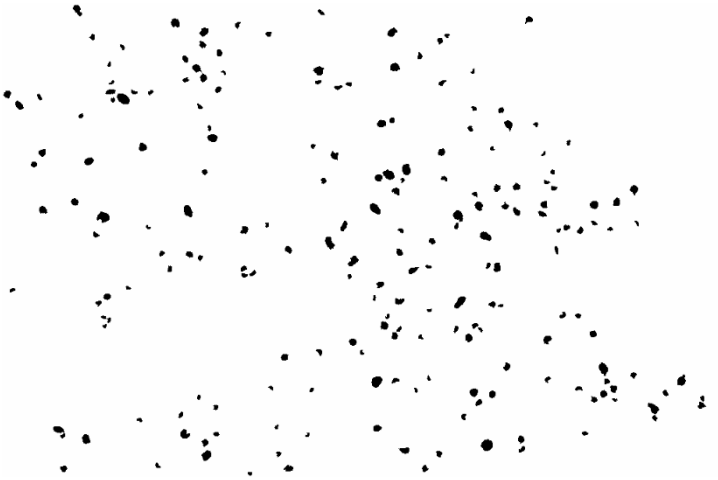

Figure S20. Using ImageJ v1.53p software, the following particles were counted/extracted from Photo No. 61559, shown above, using default threshold settings and the included 'Analyze Particles' function. The particles identified by ImageJ were used to create the diameter distribution plots of the aggregates in Figure 4.

Section 7 Dynamic Light Scattering

In preparation for DLS measurements, the refractive indices of dioxane-water mixtures were obtained using a Bausch & Lomb manual refractometer, providing the following data.

f_w (%)	0	10	20	30	40	50	60	70	80	90	100
η	1.4205	1.4150	1.4085	1.4020	1.3945	1.3870	1.3795	1.3710	1.3640	1.3445	1.332

Dynamic light scattering experiments were performed on a Malvern Nano ZS Zetasizer set to 25 °C, using a 633 nm laser set to 173° backscattering. 1 mL of aggregate suspension was prepared in the usual way, then placed in quartz cuvettes and allowed to equilibrate for 120 additional seconds. The runs each took 10 seconds, data was averaged over 10 runs and 3 separate measurements were collected of each sample, then the experiment was repeated 3 times at each f_w for a total of 9 data collections per f_w. Although experiments were conducted on **1** suspensions of f_w 0-40%, the data were flagged as poor by the internal quality reporting due to the lack of light scattering, and thus are not shown.

Table S2. Summary of Z-averages and polydisperity Indices (PdI) for **1** aggregate suspensions measured by DLS

f_w (%)	Mean Z-average (d. nm)	Std. dev (nm)	Mean PdI	Std. dev
50	367	27	0.074	0.041
60	340	19	0.104	0.046
70	292	36	0.173	0.058
80	87	8	0.155	0.033
90	67	10	0.166	0.018

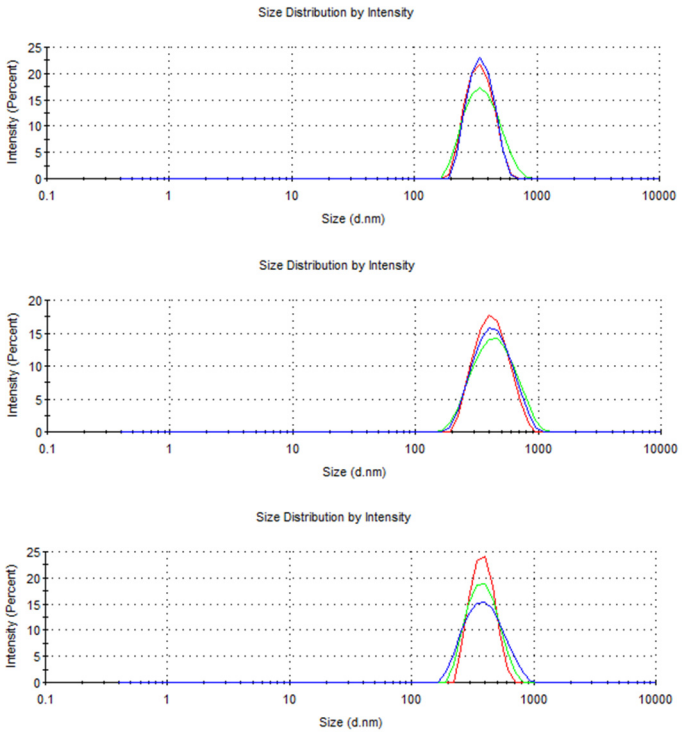

Z-averages (nm)
329
337
340
375
364
367
394
398
400

Figure S21. Intensity size charts and Z-averages of **1** aggregates formed from solution with f_w 50%.

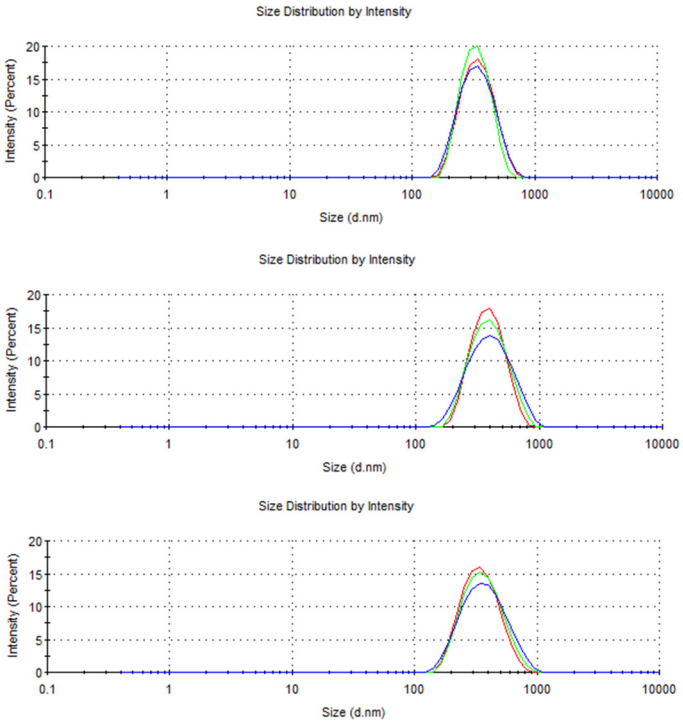

Z-averages (nm)
325
318
318
363
370
356
337
335
336

Figure S22. Intensity size charts and Z-averages of **1** aggregates formed from solution with f_w 60%.

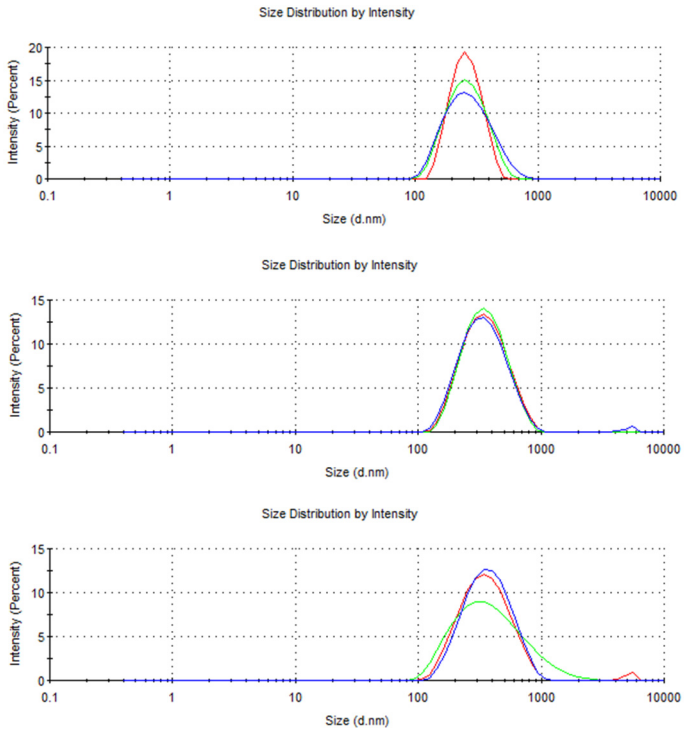

Z-averages (nm)
245
243
246
317
312
313
320
315
316

Figure S23. Intensity size charts and Z-averages of **1** aggregates formed from solution with f_w 70%.

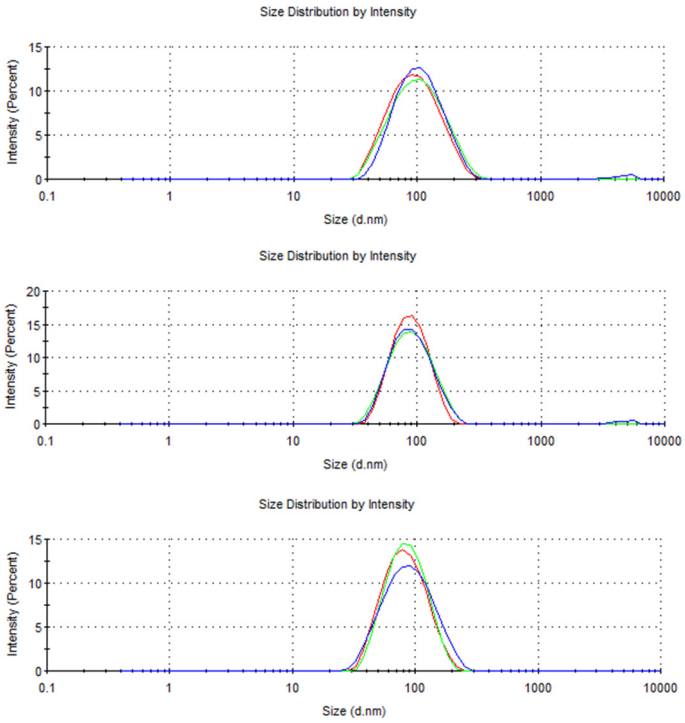

Z-averages (nm)
87
90
95
92
95
95
75
78
79

Figure S24. Intensity size charts and Z-averages of **1** aggregates formed from solution with f_w 80%.

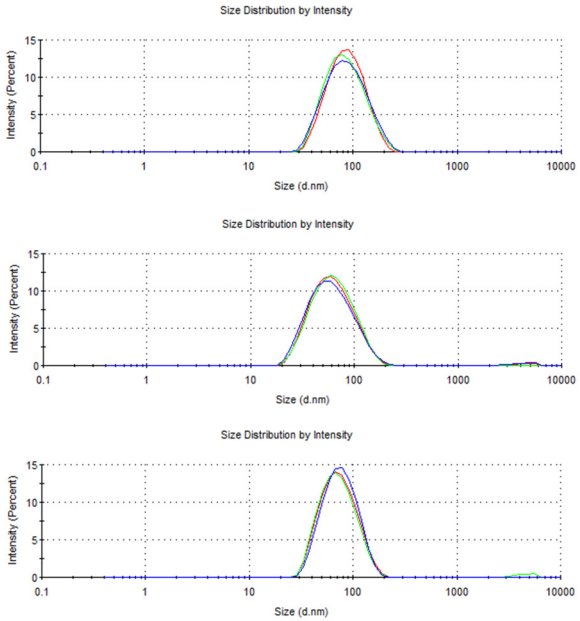

Z-averages (nm)
78
78
78
55
55
54
67
67
67

Figure S25. Intensity size charts and Z-averages of **1** aggregates formed from solution with f_w 90%.

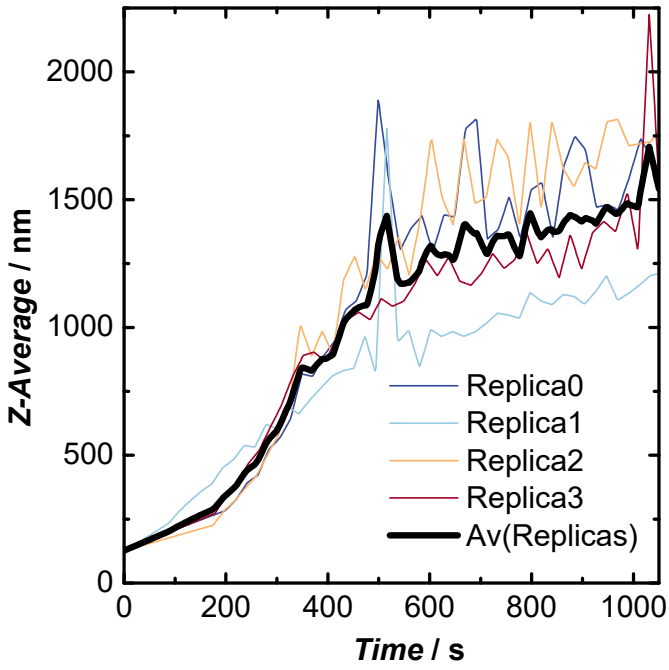

Figure S26. DLS assessment of Z-average (diameter) magnitude change as a function of time to follow the temporal ripening of the particles over approximately 20 minutes once water and **1** was added to f_w = 90% to bring the final f_w to 60% at constant 10 μM **1** concentration.

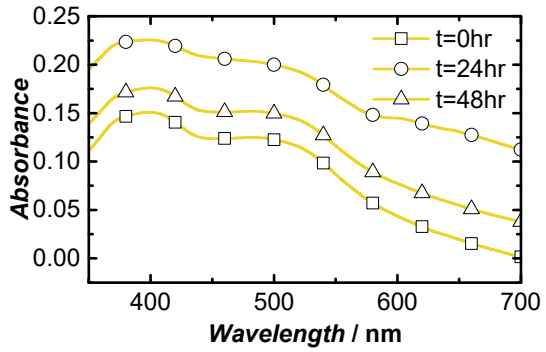

Figure S27.a Non-normalized absorbance plots of 10 μM f_w 60% suspension of **agg-Y** aged at room temperature over 48 hours complementary to Figure 5 of main manuscript.

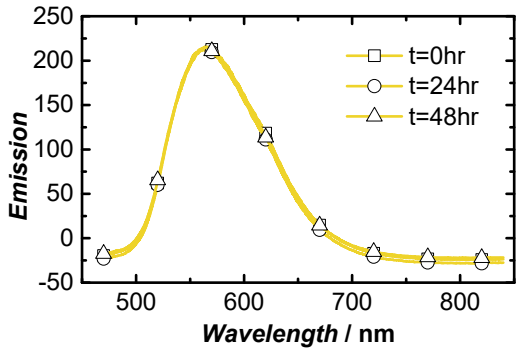

Figure S27.b Non-normalized emission plots (λ_{exc}= 460 nm) of 10 μM f_w 60% suspension of **agg-Y** aged at room temperature over 48 hours complementary to Figure 5 of main manuscript.

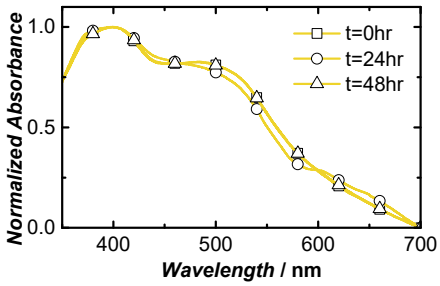

Figure S28. Normalized absorbance plots of 10 μM f_w 60% suspension of **agg-Y** aged at room temperature over 48 hours complementary to Figure 5 of main manuscript.

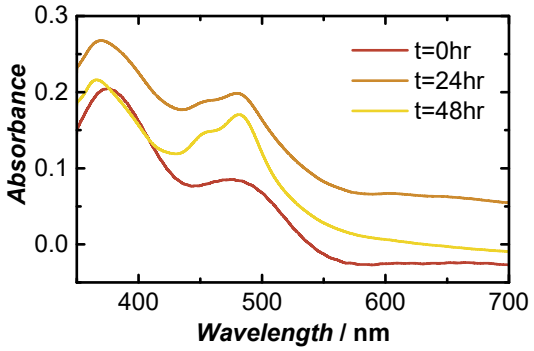

Figure S29.a Non-normalized absorbance plots of 10 μM f_w 80% suspension of **agg-O** aged at room temperature over 48 hours complementary to Figure 5 of main manuscript.

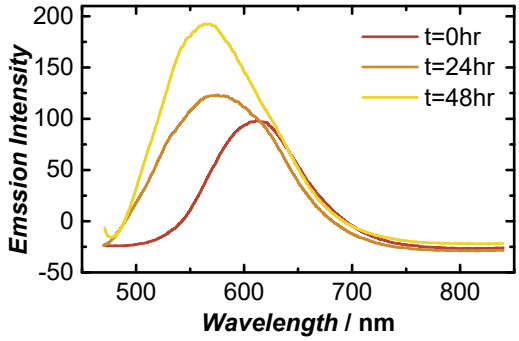

Figure S29.b Non-normalized emission plots (λ_{exc}= 460 nm) of 10 μM f_w 80% suspension of **agg-O** aged at room temperature over 48 hours complementary to Figure 5 of main manuscript.

Section 9 Thermal Treatment Experiments

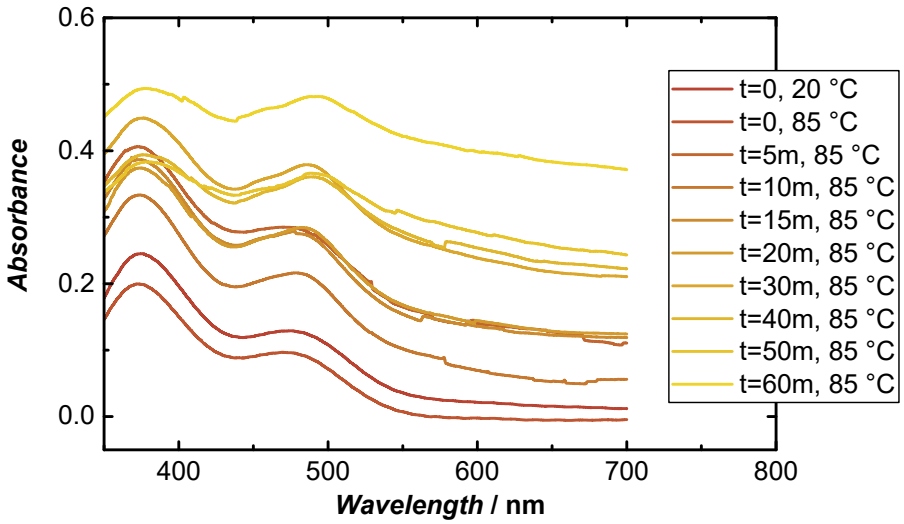

Figure S30. Non-normalized absorbance plots of 10 μM f_w 90% suspension of **agg-O** heated at 85 °C 60 minutes complementary to Figure 6 of main manuscript.

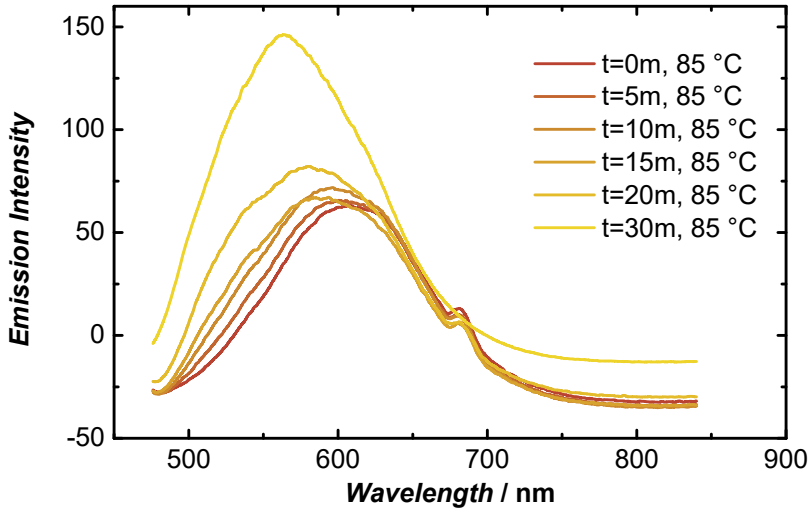

Figure S31. Non-normalized emission plots (λ_{exc}= 460 nm) of 10 μM f_w 90% suspension of **agg-O** heated at 85 °C 30 minutes complementary to Figure 6 of main manuscript.

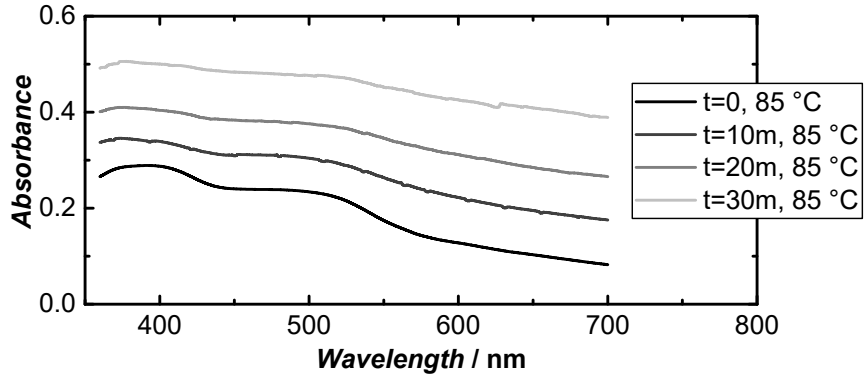

Figure S32. Non-normalized absorbance plots of 10 μM f_w 60% suspension of **agg-Y** heated at 85 °C 30 minutes complementary to Figure 6 of main manuscript.

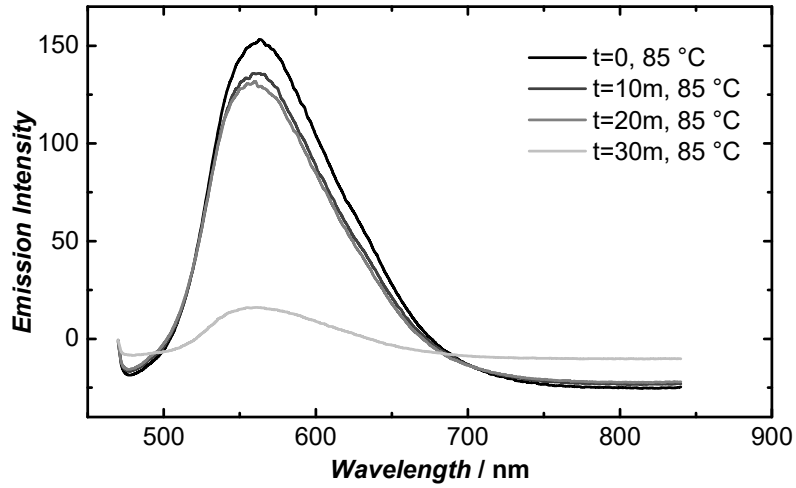

Figure S33. Non-normalized emission plots (λ_{exc}= 460 nm) of 10 μM f_w 60% suspension of **agg-Y** heated at 85 °C 30 minutes complementary to Figure 6 of main manuscript.

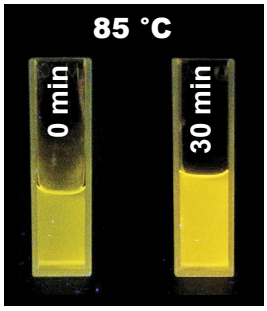

Figure S34. Photographs of emission of **agg-Y** suspension after heating f_w = 60% at constant 10 μM of **1** under 365 nm light.

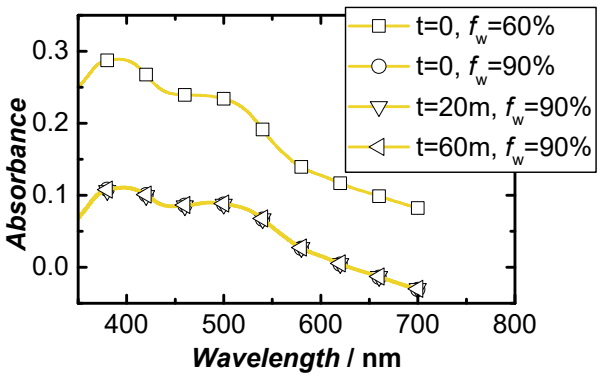

Figure S35.a Evolution over time in minutes of absorbance spectra of a 10 μM f_w 60% suspension of **agg-Y** brought to f_w 90% at constant concentration of **1**, complementary to Figure 7 of main manuscript.

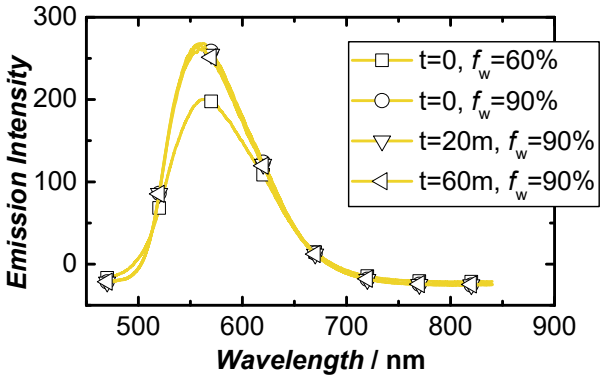

Figure S35.b Evolution over time in minutes of emission spectra (λ_{exc}= 460 nm) of a 10 μM f_w 60% suspension of b brought to f_w 90% at constant concentration of **1**, complementary to Figure 7 of main manuscript.

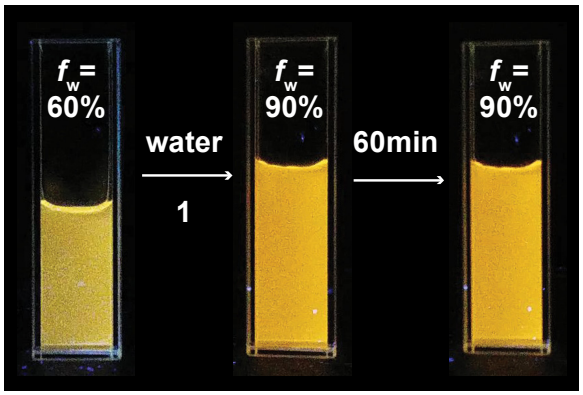

Figure S36.a Photographs of emission of **agg-Y** suspension after changing f_w from 60% to 90% at constant 10 μM of **1** under 365 nm light.

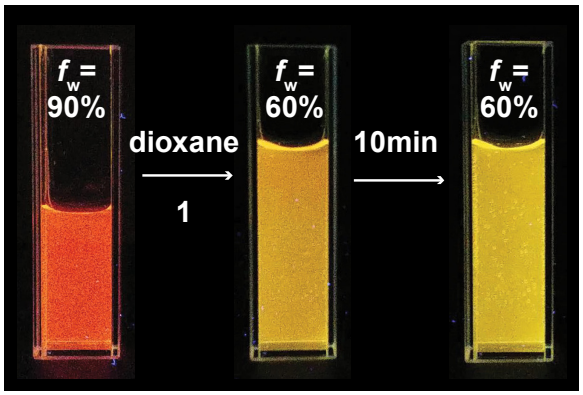

Figure S36.b Photographs of emission of **agg-O** suspension after changing f_w from 90% to 60% at constant 10 μM of **1** under 365 nm light.

Section 11 Time-resolved emission

Emission lifetimes were measured using a time-correlated single-photon counting (TCSPC) card on an Edinburgh FLS980 fluorimeter. The sample was excited using a 404.8 nm pulsed LED laser with a pulse width of 58.4 ps. Excitation and emission step increments were set to 1 nm, and both excitation and emission bandwidths were set to 2 nm. Ten thousand counts were collected for each sample to obtain the decay trace, which was then subjected to a reconvolution fit using the Edinburgh F900 software to obtain the emission lifetimes.

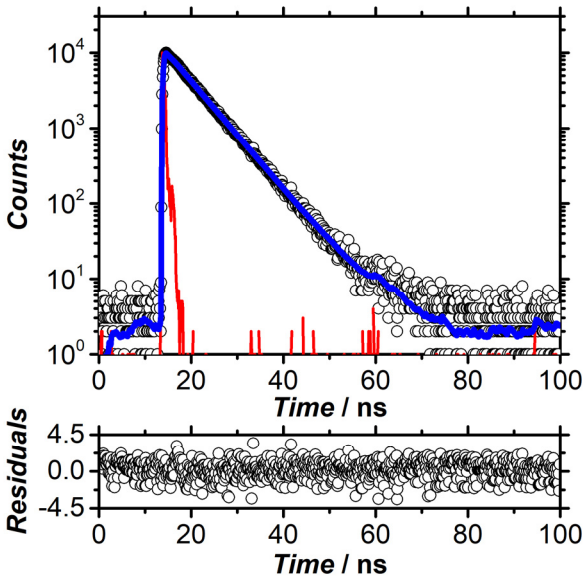

Figure S37. Emission decay (λ_{exc}= 405 nm) from excited state of **1** (10 mM) in dioxane containing f_w 0% monitoring at 560 nm (black circles), instrument response factor (red line), best fit line (blue line) and residuals plot.

$$Counts = A + B_1 e^{(-t/\tau_1)}$$

τ1	6.07	B1	0.21

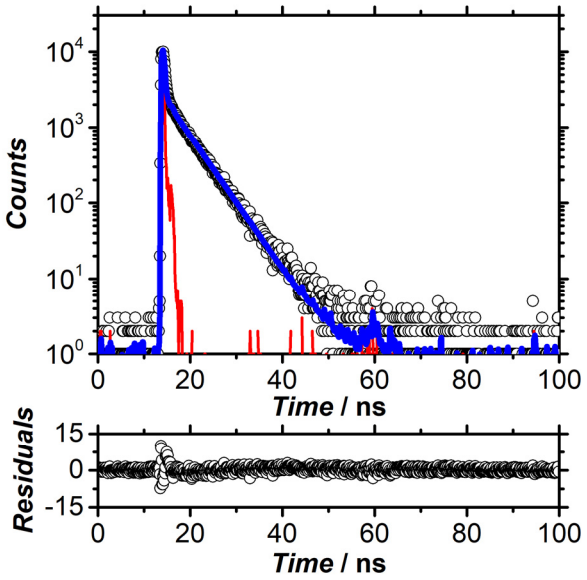

$$Counts = A + B_1 e^{(-t/\tau_1)}$$

τ1 4.91 B1 0.05

Figure S38. Emission decay (λ_{exc}= 405 nm) from excited state of **1** (10 mM) in dioxane containing f_w 10% monitoring at 560 nm (black circles), instrument response factor (red line), best fit line (blue line) and residuals plot.

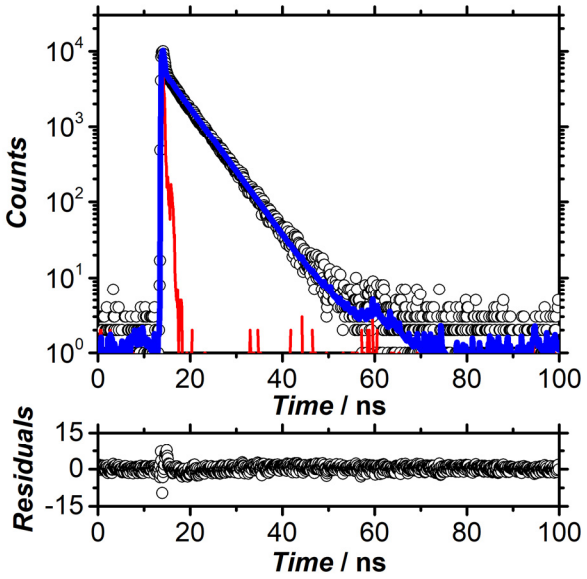

$$Counts = A + B_1 e^{(-t/\tau_1)}$$

τ1 5.16 B1 0.11

Figure S39. Emission decay (λ_{exc}= 405 nm) from excited state of **1** (10 mM) in dioxane containing f_w 20% monitoring at 560 nm (black circles), instrument response factor (red line), best fit line (blue line) and residuals plot.

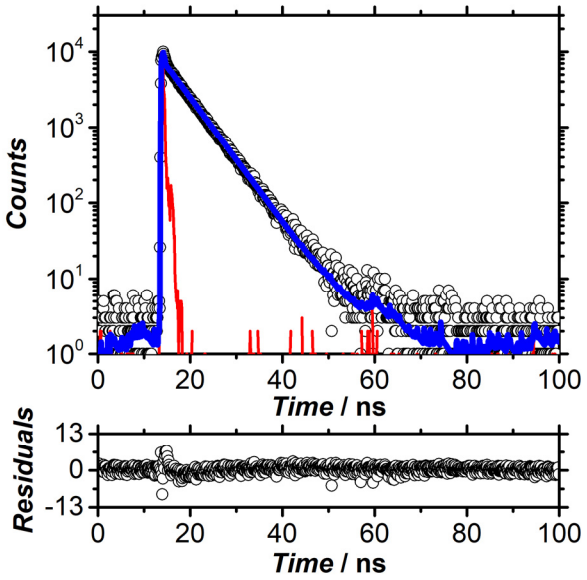

$$Counts = A + B_1 e^{(-t/\tau_1)}$$

τ1 5.27 B1 0.15

Figure S40. Emission decay (λ_{exc}= 405 nm) from excited state of **1** (10 mM) in dioxane containing f_w 30% monitoring at 560 nm (black circles), instrument response factor (red line), best fit line (blue line) and residuals plot.

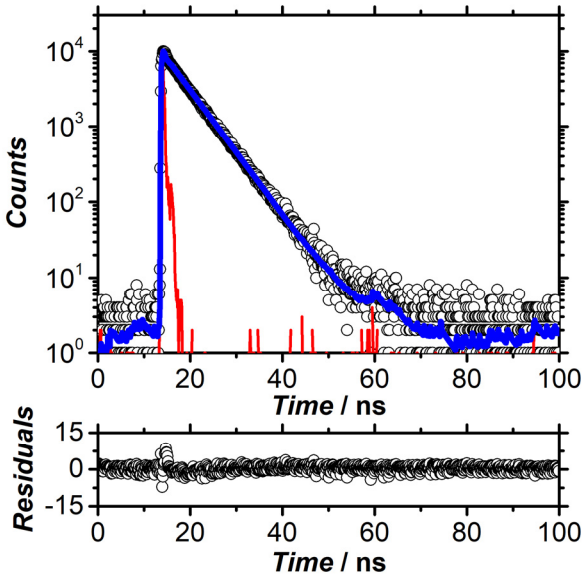

$$Counts = A + B_1 e^{(-t/\tau_1)}$$

τ1 5.24 B1 0.18

Figure S41. Emission decay (λ_{exc}= 405 nm) from excited state of **1** (10 mM) in dioxane containing f_w 40% monitoring at 560 nm (black circles), instrument response factor (red line), best fit line (blue line) and residuals plot.

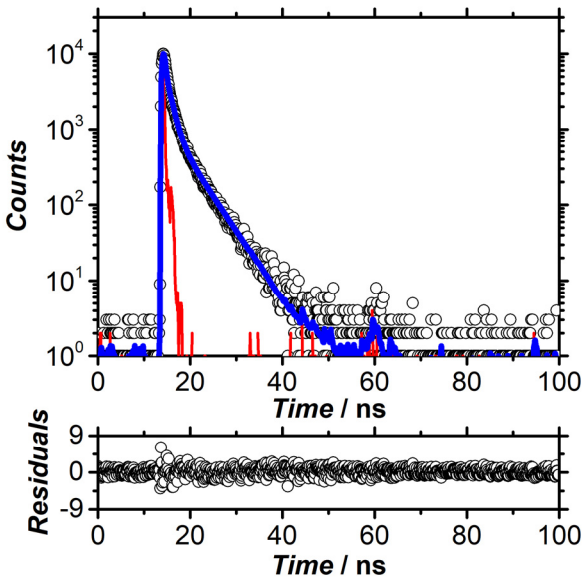

$$Counts = A + B_1 e^{(-t/\tau_1)} + B_2 e^{(-t/\tau_2)}$$

τ1	1.14	B1	0.15
τ2	4.7	B2	0.02

Figure S42. Emission decay (λ_{exc}= 405 nm) from excited state of **1** (10 mM) in dioxane containing f_w 50% monitoring at 560 nm (black circles), instrument response factor (red line), best fit line (blue line) and residuals plot.

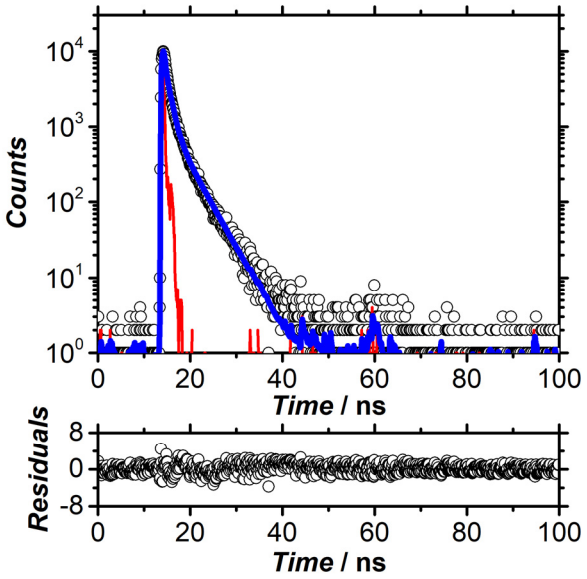

$$Counts = A + B_1 e^{(-t/\tau_1)} + B_2 e^{(-t/\tau_2)}$$

τ1	0.95	B1	0.18
τ2	3.97	B2	0.03

Figure S43. Emission decay (λ_{exc}= 405 nm) from excited state of **1** (10 mM) in dioxane containing f_w 60% monitoring at 560 nm (black circles), instrument response factor (red line), best fit line (blue line) and residuals plot.

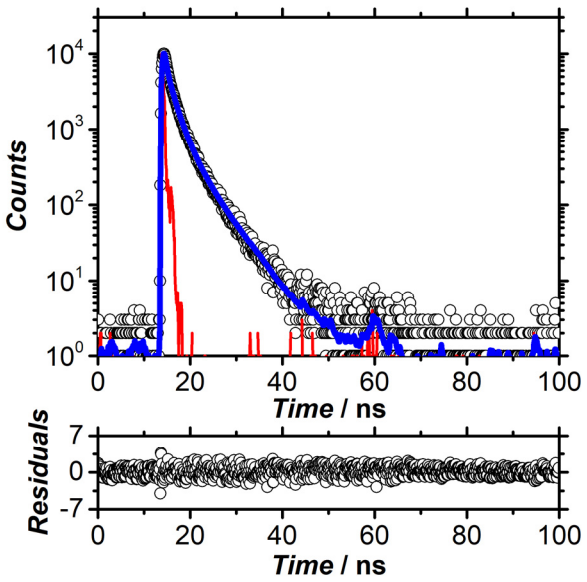

Figure S44. Emission decay (λ_{exc}= 405 nm) from excited state of **1** (10 mM) in dioxane containing f_w 60% monitoring at 613 nm (black circles), instrument response factor (red line), best fit line (blue line) and residuals plot.

$$Counts = A + B_1 e^{(-t/\tau_1)} + B_2 e^{(-t/\tau_2)}$$

τ1	1.96	B1	0.12
τ2	5.28	B2	0.02

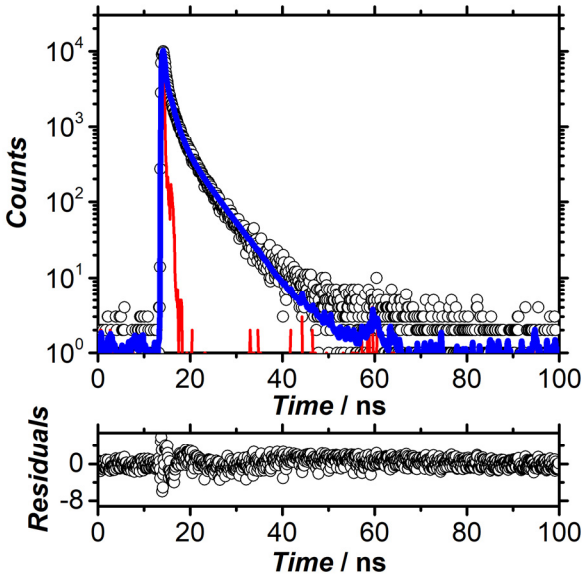

Figure S45. Emission decay (λ_{exc}= 405 nm) from excited state of **1** (10 mM) in dioxane containing f_w 70% monitoring at 560 nm (black circles), instrument response factor (red line), best fit line (blue line) and residuals plot.

$$Counts = A + B_1 e^{(-t/\tau_1)} + B_2 e^{(-t/\tau_2)}$$

τ1	1.34	B1	0.1
τ2	5.29	B2	0.02

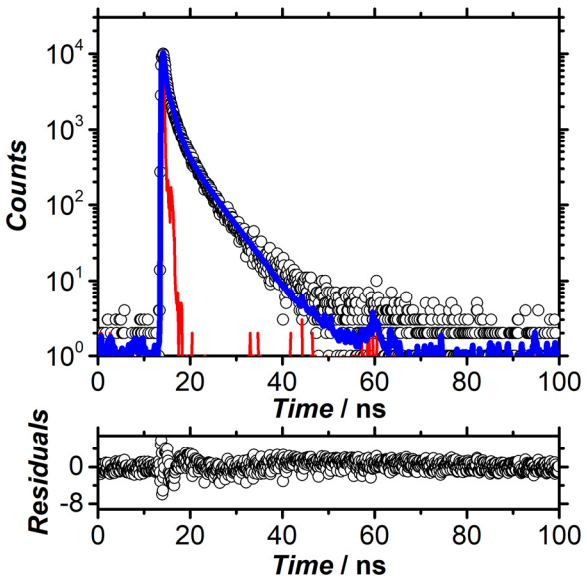

Figure S46. Emission decay (λ_{exc}= 405 nm) from excited state of **1** (10 mM) in dioxane containing f_w 70% monitoring at 613 nm (black circles), instrument response factor (red line), best fit line (blue line) and residuals plot.

$$Counts = A + B_1 e^{(-t/\tau_1)} + B_2 e^{(-t/\tau_2)}$$

τ1	2.14	B1	0.1
τ2	5.79	B2	0.01

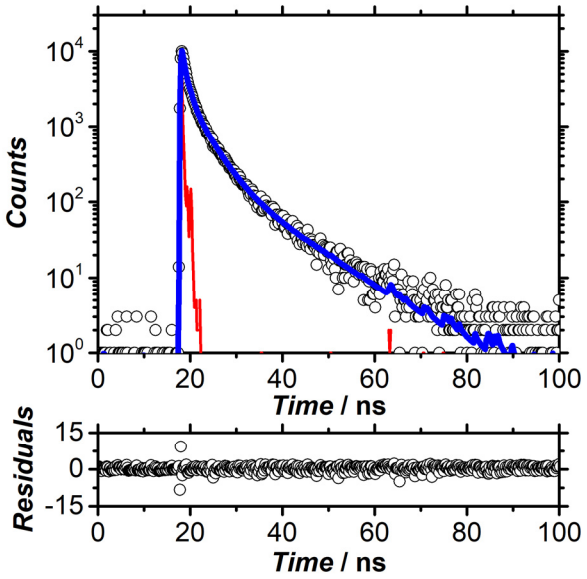

Figure S47. Emission decay (λ_{exc}= 405 nm) from excited state of **1** (10 mM) in dioxane containing f_w 80% monitoring at 613 nm (black circles), instrument response factor (red line), best fit line (blue line) and residuals plot.

$$Counts = A + B_1 e^{(-t/\tau_1)} + B_2 e^{(-t/\tau_2)} + B_3 e^{(-t/\tau_3)}$$

τ1	0.91	B1	0.35
τ2	3.56	B2	0.12
τ3	11.08	B3	0.01

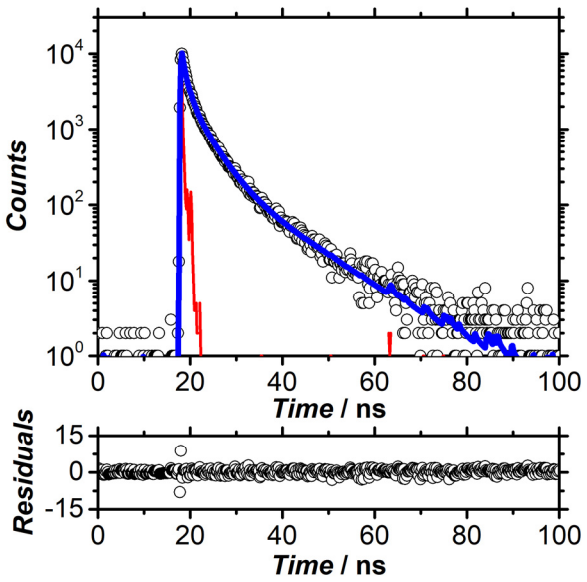

$$Counts = A + B_1 e^{(-t/\tau_1)} + B_2 e^{(-t/\tau_2)} + B_3 e^{(-t/\tau_3)}$$

τ1	0.89	B1	0.32
τ2	3.63	B2	0.13
τ3	11.11	B3	0.02

Figure S48. Emission decay (λ_{exc}= 405 nm) from excited state of **1** (10 mM) in dioxane containing f_w 90% monitoring at 613 nm (black circles), instrument response factor (red line), best fit line (blue line) and residuals plot.

Quantum yields and radiative rate constants were used to determine non-radiative rate constants using the following formula:

$$\Phi_{em} = \frac{k_r}{k_r + k_{nr}}$$

Table S3. Summary of radiative and non-radiative rate constants as a function of water fraction.

f_w / %	k_r / s^{-1}	k_{nr} / s^{-1}
0	1.65×10^8 (560 nm)	5.33×10^8 (560 nm)
10	2.04×10^8 (560 nm)	4.12×10^{10} (560 nm)
20	1.94×10^8 (560 nm)	8.06×10^{10} (560 nm)
30	1.90×10^8 (560 nm)	1.26×10^{11} (560 nm)
40	1.91×10^8 (560 nm)	1.43×10^{11} (560 nm)
50	1.09×10^9 (560 nm)	5.74×10^{10} (560 nm)
60	1.30×10^9 (560 nm)	7.65×10^{10} (560 nm)
	7.00×10^8 (613 nm)	4.10×10^{10} (613 nm)
70	9.35×10^8 (560 nm)	5.49×10^{10} (560 nm)
	6.40×10^8 (613 nm)	3.76×10^{10} (613 nm)
80	1.47×10^9 (613 nm)	1.10×10^{11} (613 nm)
90	1.49×10^9 (613 nm)	2.01×10^{11} (613 nm)

Section 12 Polymorphs orange and yellow crystal structures and thermal properties.

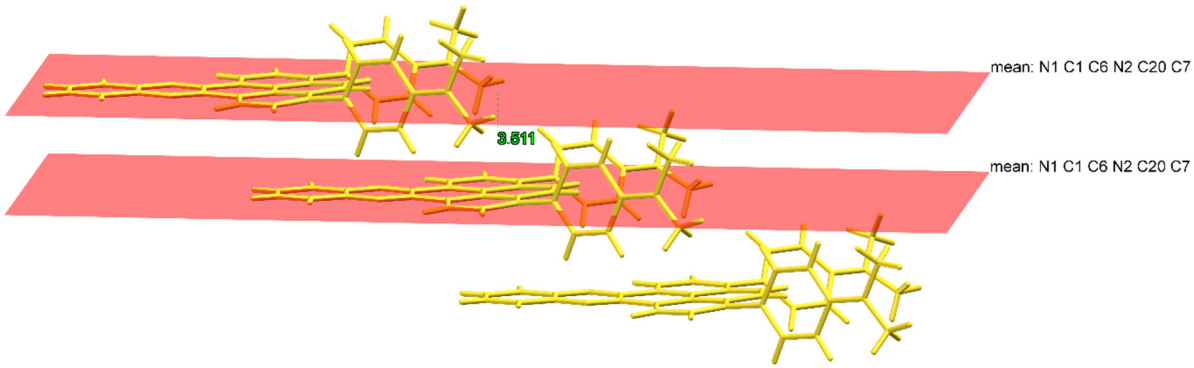

Figure S49. Packing image of **morph-Y** highlighting the intermolecular aryl-aryl interaction distance of 3.51 Å. Single crystal data is available in CCDC 1959739 and has been reported previously.[1]

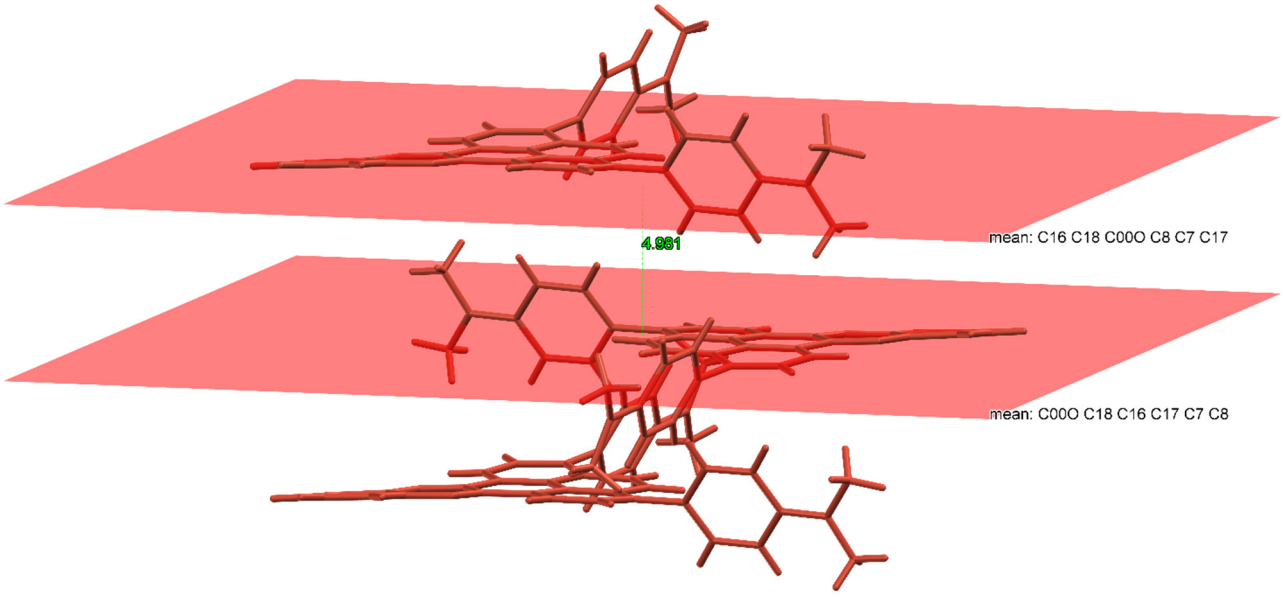

Figure S50. Packing image of **morph-O** highlighting the large intermolecular spacing between pi-conjugated surfaces of 4.98 Å. Single crystal data is available in CCDC 1959741 and has been reported previously.[1]

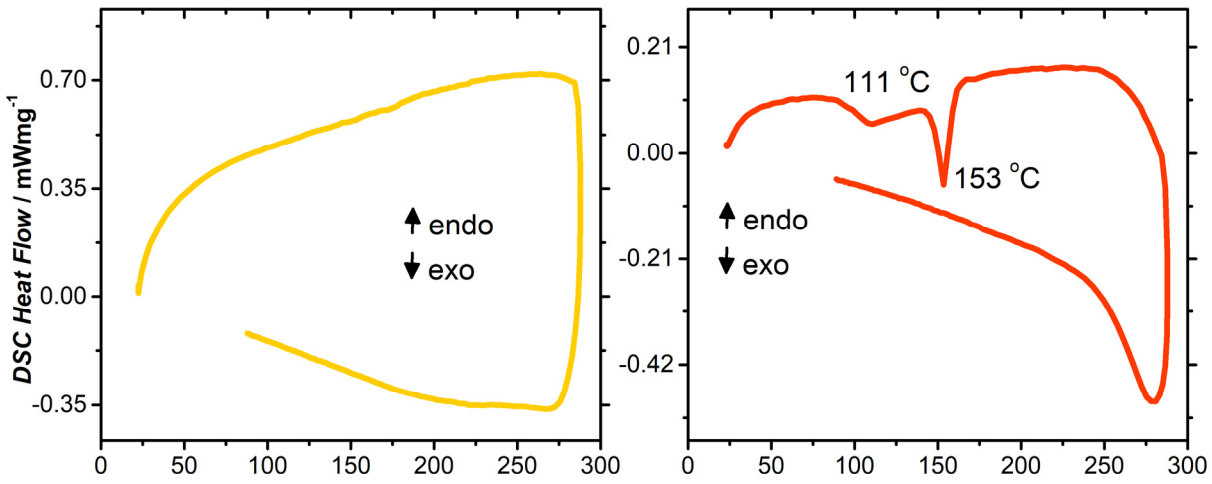

Figure S51. Differential scanning calorimetry thermogram of **morph-Y** and **morph-O**, which have been reported previously.[1]

Section 13 References

1D. T. Hogan, B. S. Gelfand, D. M. Spasyuk and T. C. Sutherland, *Mater. Chem. Front.*, 2020, **4**, 268–276.
2A. T. R. Williams, S. A. Winfield and J. N. Miller, *Analyst*, 1983, **108**, 1067–1071.
3G. A. Reynolds and K. H. Drexhage, *Opt. Commun.*, 1975, **13**, 222–225.
4N. Macia, V. Kabanov, M. Côté-Cyr and B. Heyne, *J. Phys. Chem. Lett.*, 2019, **10**, 3654–3660.
5N. Macia, V. Kabanov and B. Heyne, *J. Phys. Chem. C*, 2020, **124**, 3768–3777.
6V. Kabanov and B. Heyne, *ACS Appl. Nano Mater.*, 2020, **3**, 8126–8137.